

Analytical Methods

Accepted Manuscript



This is an *Accepted Manuscript*, which has been through the Royal Society of Chemistry peer review process and has been accepted for publication.

Accepted Manuscripts are published online shortly after acceptance, before technical editing, formatting and proof reading. Using this free service, authors can make their results available to the community, in citable form, before we publish the edited article. We will replace this *Accepted Manuscript* with the edited and formatted *Advance Article* as soon as it is available.

You can find more information about *Accepted Manuscripts* in the [Information for Authors](#).

Please note that technical editing may introduce minor changes to the text and/or graphics, which may alter content. The journal's standard [Terms & Conditions](#) and the [Ethical guidelines](#) still apply. In no event shall the Royal Society of Chemistry be held responsible for any errors or omissions in this *Accepted Manuscript* or any consequences arising from the use of any information it contains.

Switching the recognition preference of thiourea derivative by replacing Cu²⁺: Spectroscopic characteristic of aggregation-induced emission and the mechanism studies for recognition of Hg(II) in aqueous solution

Aizhi Wang, Yunxu Yang *, Feifei Yu, Lingwei Xue, Biwei Hu, Yajun Dong, Weiping Fan

Department of Chemistry and Chemical Engineering, School of Chemistry and Biological Engineering, University of Science and Technology Beijing,

Beijing 100083, China

Tel: +86-010-62333871

Email: yxyang@ustb.edu.cn

Abstract:

A thiourea functionalized π -conjugated cyanostilbene derivative of (Z)-N-((4-(2-cyano-2-phenylvinyl)phenyl)carbamothioyl)acetamide (CN-S) has been designed, synthesized and characterized by the standard spectroscopic analyses. CN-S exhibited excellent AIE property in DMSO/water mixture with high water fraction and showed highly selective and sensitive recognition towards Cu²⁺ and Hg²⁺ ions with great fluorescence changes. By addition of Cu²⁺ to CN-S, it displayed a turn-off fluorescent response and generated a Cu-CN-S complex which was also confirmed by the theoretical calculation. However, the complex of Cu-CN-S showed turn-on fluorescent response to Hg²⁺ with high selectivity and sensitivity because of the desulfurization reaction. In addition, there is a good linear relationship ($R^2=0.9966$) between the fluorescence intensity and the concentration of Hg²⁺. The detection limit of Hg²⁺ is 45 nM. By this novel strategy, this single molecular (CN-S) can be used as

fluorescent sensor to detect Hg^{2+} specifically.

Keywords: Fluorescent chemsensor; Aggregation-induced emission; Hg^{2+} ion; Thiourea derivative.

1 Introduction

Heavy and transition metal (HTM) ions contamination can produce extremely toxic impact on human health and environment, thus a serious concern has been remained across the world for decades.¹⁻³ Although transition-metal ion Cu^{2+} is an active part in a large variety of enzymes, including superoxide dismutase, cytochrome oxidase and tyrosinase,^{4,9} it exhibits toxicity associated with neurodegenerative diseases such as Alzheimer's, Prion, Wilson and Menkes disease¹⁰⁻¹⁵ under overloading conditions. Similarly, Hg^{2+} ion can cause serious environmental and health issues because of its extreme toxicity and bioaccumulation.¹⁶⁻²⁰ The solvated divalent mercuric ion is the most common and stable form among mercury pollution due to its high water solubility. Thus, obtaining a new onsite detection method for Cu^{2+} and Hg^{2+} in view of the cost effective, rapid, facile, sensitive, selective and applicable is an important goal.

Among various proposed methods previously, fluorescent chemosensors have received great attentions. It exhibits good potential applications for the detection and quantification of metal ions in the field of molecular biology as well as environment et al. Furthermore, fluorescence turn-on sensors, the fluorescence intensity of which increases upon the amount of HTM ions, are believed to be resistant to interferences of other ions, making it easy to detect and quantify with the advantages of onsite and

1
2
3
4 realtime detection.²¹ Numerous fluorescent probes have been reported for sensing of
5
6 Cu^{2+} , such as rhodamine derivatives,²²⁻²⁵ two-photon probes,²⁶ silica nanoparticle²⁷
7
8 and Schiff base.²⁸ Likewise, several probes have been designed for Hg^{2+} , like indole,²⁹
9
10 sulfonamide,³⁰ triazole-based dansy,³¹ rhodamine derivatives³² and so on. However,
11
12 most of them have certain disadvantages of low solubility in aqueous solution, low
13
14 sensitivity and selectivity, time-consuming, laborious synthesis and the turn-off
15
16 response. Moreover, most fluorophores have suffered from fluorescence quenching in
17
18 high concentration or solid state due to π - π stacking interaction. This is an annoying
19
20 phenomenon, which is commonly known as aggregation-caused-quenching (ACQ).
21
22 To overcome the ubiquitous ACQ effect, a latest breakthrough in the synthesis of
23
24 π -conjugated organic polyenes with intriguing aggregation-induced emission (AIE)
25
26 phenomenon has attracted special attention.³³⁻³⁶ This kind of molecule can reduce the
27
28 no-radiative energy dissipation pathways and favor the radiative decay of exciton in
29
30 its high concentration or solid state, which provides an efficient way to resolve
31
32 notorious problem of ACQ and has been successfully applied in bioprobes,
33
34 stimuli-responsive nanomaterials, fluorescence sensor, cell imaging and active layers
35
36 in the construction of efficient organic light emitting diodes.³⁷⁻³⁹ Thus, it will be a
37
38 fascinating work for us to develop an opposite ACQ effect material so as to achieve
39
40 high emission in aggregated or solid state.
41
42
43
44
45
46
47
48
49
50
51
52
53
54

55 Herein, we provided a novel concept and synthesized a fluorescent probe,
56
57 (Z)-N-((4-(2-cyano-2-phenylvinyl)phenyl)carbamothioyl)acetamide (**CN-S**), based on
58
59 π -conjugated cyanostilbene derivatives which exhibits the classical AIE effect.⁴⁰⁻⁴³
60

The synthetic pathway of **CN-S** was shown in scheme 1. It was interesting that the fluorescence of **CN-S** can be completely quenched by Cu^{2+} when we did the test, revealing that there is an effective coordination between **CN-S** and Cu^{2+} ions. However, significant fluorescence enhancement can be observed from the transformation of **Cu-CN-S** to (Z)-N-((4-(2-cyano-2-phenylvinyl)phenyl)carbamoyl)-thiophenylacetamide (**CN-O**) based on Hg^{2+} -induced desulfurization reaction. It is an irreversible fluorescence probe with lower detection limit, higher selectivity and sensitivity than the reversible ones.⁴⁴⁻⁴⁹ Therefore, **CN-S** is a satisfactory fluorescence probe for Hg^{2+} with highly selective and sensitive in aqueous solution.

(Scheme 1 is inset here)

2. Experimental section

2.1. Reagents and apparatus

All reagents and solvents available from commercial suppliers were analytical reagent (AR) grade and were used without further purification unless otherwise stated. The water used for investigating was distilled prior to use. Benzylcyanide and *p*-nitrobenzaldehyde were purchased from Alfa Aesar. The certified reference material of the standard solution of Hg^{2+} was purchased from General Research Institute for Nonferrous Metals, China and the certificate information was shown in Table S1. Stock solutions of interfering metal ions (2.5 mM) were prepared from eighteen kinds of metal ions, including Li^+ , Na^+ , K^+ , Mg^{2+} , Ca^{2+} , Al^{3+} , Fe^{2+} , Fe^{3+} , Mn^{2+} , Co^{2+} , Ni^{2+} , Pb^{2+} , Zn^{2+} , Sn^{2+} , Ag^+ , Cd^{2+} , Ba^{2+} and Cr^{3+} . Stock solutions of Cu^{2+} and Hg^{2+} (2.5 mM)

were prepared in deionized water. The probe stock solution (10 mM) was obtained by dissolving **CN-S** (32.1 mg) in DMSO (10 ml) at room temperature. Phosphate buffer solutions (PBS) were prepared by combining proper amounts of NaH₂PO₄ and NaOH, and adjusted by a pH meter. Purification of reaction products was carried out by flash chromatography using silica gel (300–400 mesh, Branch of Qingdao Haiyang Chemical Co., LTD).

FT-IR spectra were obtained in KBr discs on a Shimadzu IR-8400S spectrophotometer in the region of 4000–400 cm⁻¹. ¹H NMR and ¹³C NMR spectra were measured on a Varian Gemin-400 MHz spectrometer with chemical shifts reported in ppm (in DMSO-d₆, TMS as interna standard, and the multiplicities were expressed as follows: *s* = single, *d* = double, *t* = triplet, *m* = multiplet). ESI-MS spectra were recorded on Bruker spectrometers. All UV-Visible and fluorescence spectra in this work were performed in Pgeneral TU-1901 and Hitachi F-4500 fluorescence spectrometers. All pH values were carried out on a Model pHs-3C pH meter (Shanghai, China). Analytical TLC was carried out on silica gel plates (HSGF254, 0.2mm, Yantai Chemical Industry Research Institute). Melting points were taken on RD-II melting point apparatus (uncorrected, Tainjin Xintianguang Instrument Company).

2.2. Synthesis

The synthetic route of compound **CN-S** was shown in Scheme 1.

Synthesis of (Z)-3-(4-aminophenyl)-2-phenylacrylonitrile (compound-2)

Compound-2 was synthesized by the procedure reported in the literature.⁵⁰

Sodium (0.057 g, 0.0025 mol) was added to methanol (10 mL) in a 50 ml one-neck flask, heat and stirred until the sodium disappeared. Then benzyl cyanide (0.58 g, 0.005 mol) and *p*-nitrobenzaldehyde (0.75 g, 0.005 mol) were added. The mixture was stirred at room temperature for about 2 h and a lot of yellow precipitates formed during reaction. Filtered, the solid was washed by methanol and water for three times to give light yellow compound **1** (1.16 g, 93%).

Compound **1** (1.25 g, 0.005 mol), ethanol (20 mL) and stannous chloride dihydrate ($\text{SnCl}_2 \cdot 2\text{H}_2\text{O}$, 5.6 g, 0.025 mol) and the mixture was refluxed for about 0.5h. Neutralized with saturated Na_2CO_3 to weak basicity, diluted with water (about 25 mL), and extracted with chloroform. The combined extracted organic phase was dried over anhydrous sodium sulfate, filtered, and evaporated to dry by rotary evaporator to give a yellow solid (1.05g, 95%).

Synthesis of (Z)-N-((4-(2-cyano-2-phenylvinyl)phenyl)carbamothioyl)acetamide (CN-S)

A solution of sodium thiocyanate (182 mg, 2.25 mmol) in acetonitrile (5 mL) was stirred at room temperature (rt), acetyl chloride (0.08 mL, 1.13 mmol) was added dropwise. The mixture was refluxed for 1h and then cooled to rt. Then, (Z)-3-(4-aminophenyl)-2-phenylacrylonitrile (62.0 mg, 0.282 mmol) was added to the mixture. After stirring at rt for 90 min, water (20 mL) was added, and then precipitate was obtained by filtration. The precipitate was washed with diethyl ether and water, and recrystallized from DMF/water to give the rude product as yellow crystals. The

yellow crystals was purified by column chromatography (EtOAc/petroleum ether = 1:5 as eluent) to afford **CN-S** as a pale yellow solid (75.1 mg, 83%). mp 215-217°C. elemental analysis: Calcd for: $C_{18}H_{15}N_3OS$, C, 67.27; H, 4.70; N, 13.07; S, 9.98; found: C, 68.95; H, 4.11; N, 12.68; S, 10.06%. IR (KBr) ν : 3441, 3185, 3030, 2215, 1689, 1591.65, 1534, 1336, 1156, 764 cm^{-1} ; 1H NMR (400 MHz, DMSO- d_6) δ (ppm): 12.69 (s, 1H), 11.59 (s, 1H), 8.04 (s, 1H), 7.97 (d, $J=8.4$ Hz, 2H), 7.86 (d, $J=8.4$ Hz, 2H), 7.76 (d, $J=7.2$ Hz, 2H), 7.54-7.45 (m, 5H), 2.16 (s, 3H); ^{13}C NMR (DMSO- d_6) δ (ppm): 179.04, 173.29, 142.47, 140.04, 134.24, 131.73, 130.09, 129.67, 126.67, 126.21, 124.35, 118.42, 110.24, 24.32; ESI-MS (m/z): calcd for: $C_{17}H_{12}N_2O_3 [M+Na]^+$ 344.08, found 344.19.

2.3. Analytical procedure

To characterize the AIE property of **CN-S**, 10 μL stock solution of **CN-S** was added into 10 mL DMSO/water (10:0, 5:5, 1:9, 5:95, 1:99, 1:999, v/v, containing 50 mM NaH_2PO_4 -NaOH at pH=7.0). After mixing well, the solution was incubated at room temperature for 15 min. Quartz cuvettes with a 1 cm path length and 3 ml volume were used for all measurements.

For titration experiments of Cu^{2+} , tested solutions were prepared by placing 10 μL stock solution of **CN-S** into a test tube, diluted to 10 mL with 50 mM PBS at pH=7.0 and an appropriate amount of Cu^{2+} ions (0, 0.05, 0.1, 0.2, 0.4, 0.6, 0.8, 1.0, 1.2, 1.5 equiv.) were added; For titration experiments of Hg^{2+} , the test solution was prepared by placing 10 μL stock solution of **CN-S** and 40 μL stock solution of Cu^{2+} into a test tube, diluted to 10 mL with 50 mM PBS at pH=7.0, added appropriate amount of Hg^{2+}

ions(0, 0.1, 0.2, 0.3, 0.4, 0.5, 0.6, 0.7, 0.8, 0.9, 1.0, 1.5 equiv.). After mixing well, the solutions were allowed to stand at ambient condition for 15 min and then the fluorescence spectra were recorded.

To evaluate any possible facts which may affect the response of the fluorescence intensity caused by interfering ions, the interfering metal ions (20 μM) were added to the test solution, and then recognized metal ions (10 μM) were added to explore whether the recognition was affected by the interfering metal ions. After mixing well, the solutions were allowed to stand at ambient condition for 15 min and then the fluorescence spectra were recorded.

For detection of Hg^{2+} in real sample analysis, the concentration of Hg^{2+} in real samples was detected by the standard addition method. Real sample solutions of Hg^{2+} (6 μM) were prepared with three real water samples which contain 50 mM PBS at pH=7.0 respectively in volumetric flask. In addition, the certified standard solution of Hg^{2+} (0.5 ml) was transferred to a 500 ml volumetric flask and diluted with PBS (50 mM, pH=7.0) to the metered volume, and give a 5 μM standard solution of Hg^{2+} . Subsequently, 10 μL stock solution of **CN-S** and 40 μL stock solution of Cu^{2+} were placed into test tubes and diluted to 10 mL with the three real samples and the standard solution of Hg^{2+} respectively, and gave the test solutions. Finally, the fluorescence emission spectra were recorded.

All fluorescence spectra were recorded in the range from 400 nm to 600 nm using the 380 nm excitation wavelength. The excitation and emission bandwidths were set to 10 nm.

The Scanning Electron Microscope (SEM) images were observed and recorded on a Hitachi S-4800 instrument. Prior to TEM measurement, the suspension of **CN-S**, **CN-O** and the complex of **CN-S** and Cu^{2+} were prepared in aqueous solution (containing 0.1% DMSO). Thereafter, each sample solution was dropped onto a silicon chip and dried at ambient temperature.

3. Results and discussion

3.1. Aggregation-induced emission characteristics of **CN-S**

We first investigated the AIE behavior of **CN-S** in DMSO/water mixtures at different DMSO/water ratios, and the water content was varying in the range of 0-99.9%. From the solubility test, we know that **CN-S** is soluble in common organic solvents such as ethanol, THF and DMSO, but it is insoluble in water and hexane. As expected, **CN-S** is virtually nonluminescent when molecularly dissolved in DMSO, which was indicated by the photographs and fluorescence spectrum in Fig. 1. However, when a large amount of water was added into the solution, the emission of **CN-S** turned on and showed blue fluorescence. The fluorescence intensity of **CN-S** exhibited 6.9-fold enhancement when water content reached to 99.9%. Clearly, the emission of **CN-S** is induced by aggregate formation. To further confirm the existence of aggregate, we investigated its UV absorption spectra (Fig. 2). As water fraction was increased up to 99.9%, a level-off tail could be seen in the visible spectral region, which was commonly observed in nanoparticle suspensions. What's more, a new shoulder band (shown as the arrow) could be observed around 420 nm, which is associated with the *J*-type aggregation. In conclusion, **CN-S** exhibits AIE features.

(Fig. 1(a) is inset here)

(Fig. 1(b) is inset here)

(Fig. 2 is inset here)

3.2. pH effect on emission intensity

In order to gain the optimized analysis condition of the probe toward Cu^{2+} and Hg^{2+} , we investigated the pH effect on free **CN-S** ($10\ \mu\text{M}$), the binding ability of **CN-S** ($10\ \mu\text{M}$) toward Cu^{2+} ($10\ \mu\text{M}$) and the reactive activity of **Cu-CN-S** ($10\ \mu\text{M}$) toward Hg^{2+} ($10\ \mu\text{M}$). The fluorescence spectra were recorded. As shown in Fig. 3, the probe CN-S itself does not show fluorescence emission at high pH environment (>11) because of the 1, 4-addition reaction of OH^- to α , β -unsaturated cyano compound, which lead to destruction of the conjugate structure. There were stable changes of fluorescence intensity with the pH in the range of 1 to 9, when Cu^{2+} was added. So it is stable to detect Cu^{2+} in a large range pH (1-9). However, only in the pH range of 4-9, the progress of recognition toward Hg^{2+} would be carried out. Considering the application of samples in physiological or environmental, pH=7.0 was thus chosen as the experiment condition.

(Fig. 3 is inset here)

3.3. Fluorescence studies of **CN-S** towards metal ion

The metal ion binding properties of **CN-S** ($10\ \mu\text{M}$) towards various metal ions such as Li^+ , Na^+ , K^+ , Mg^{2+} , Ca^{2+} , Al^{3+} , Fe^{2+} , Fe^{3+} , Mn^{2+} , Cu^{2+} , Co^{2+} , Ni^{2+} , Pb^{2+} , Zn^{2+} ,

1
2
3
4 Sn^{2+} , Ag^+ , Cd^{2+} , Ba^{2+} , Cr^{3+} and Hg^{2+} were evaluated in phosphate buffer solution (PBS,
5
6
7 50 mM, pH=7.0). As shown in Fig. 4, free **CN-S** showed a broad fluorescent emission
8
9
10 at 492 nm. Obviously, the fluorescence spectra of **CN-S** in the existence of various
11
12 metal ions remain the same as that of free **CN-S** except Ag^+ , Cu^{2+} , and Hg^{2+} . When
13
14 Cu^{2+} was added to the solution of **CN-S**, a significant fluorescence quenching was
15
16 observed. However, after addition of Hg^{2+} (1.5 equiv.), a significant fluorescence
17
18 enhancement (2.4-fold) and a clearly blue-shift (22 nm) compared with free **CN-S**
19
20 could be observed. Under very careful observation, the mixture of **CN-S** with Ag^+
21
22 resulted in an obvious blue-shift, but only a slightly fluorescence enhancement
23
24 (1.05-fold) could be discovered. Therefore, **CN-S** has specific response to Cu^{2+} and
25
26 Hg^{2+} , which shows two completely opposite cases.
27
28
29
30
31
32
33
34

35 (Fig. 4 is inset here)
36
37
38

39 3.4. Fluorescence turn-off detection of Cu^{2+} based on **CN-S** 40

41 To study the quenching behavior of Cu^{2+} ions in detail, we investigated the
42
43 fluorescence titration experiments by adding Cu^{2+} successively to the diluted **CN-S**
44
45 solution in a DMSO/water mixture with 99.9% water fraction. As shown in Fig. 5,
46
47 quenching of photoluminescence was observed at a very low level of Cu^{2+} . For
48
49 example, at the very beginning, the fluorescence emission of **CN-S** decreased to 50%
50
51 of its primary emission intensity when the concentration of Cu^{2+} increased up to 0.5
52
53 μM (only 5% of the **CN-S** concentration). Upon addition of 1.0 equiv. Cu^{2+} , almost no
54
55 luminescence could be observed (Figure S4) and a perceived fluorescence color
56
57
58
59
60

change of **CN-S** was observed from blue to colorless (Fig. 5, insert). It is worth noting that **CN-S** can detect a very low concentration of Cu^{2+} . However, it is a pity that **CN-S** can't quantitatively detect Cu^{2+} .

(Fig. 5 is inset here)

3.5 The binding mechanism of **CN-S** with Cu^{2+}

As we know, Cu^{2+} ion is easy-coordinated and has a paramagnetic nature,⁵¹ which is well-known to cause fluorescence quenching. Thus, a complex of **Cu-CN-S** was likely formed by **CN-S** with Cu^{2+} ions. To confirm this fact, EDTA (5.0 equiv.) was added to the aqueous solution of **CN-S** and Cu^{2+} ions. As expected, the fluorescence restored but not strong as original (Fig. S5). This indicated that EDTA could partly catch the Cu^{2+} ions from **Cu-CN-S** and interrupt the interaction between **CN-S** and Cu^{2+} ions. In addition, a theoretical calculation was carried out in order to verify the idea. The optimized structures and orbital distributions of HOMO and LUMO energy levels of **CN-S** and **CN-O** were shown in Figure S6. The calculated energy band gap for **CN-S** is 2.712eV, which is wider than that of **CN-O** (3.535eV). The results of theoretical studies are consistent with the UV-Vis spectra (Figure S7). And the optimized structure of **Cu-CN-S** and some useful data were calculated and shown in Figure S8. Morphology of **CN-S** and the complex **Cu-CN-S** aggregates were observed by SEM as shown in Figure S9. **CN-S** would aggregate in aqueous solution (containing 0.1% DMSO) and has strong fluorescence because of the intramolecular cyclization caused by hydrogen-bond. Though **Cu-CN-S** would also aggregate, the

fluorescence intensity of **Cu-CN-S** become weak on account of intramolecular charge transfer (ICT). Thus, a mechanism depicted was supposed in scheme 2.

(Scheme 2 is inset here)

3.6 Fluorescence turn-on detection of Hg^{2+} based on **Cu-CN-S**

Fig. 6 shows the spectra of **Cu-CN-S** before and after the addition of different amounts of Hg^{2+} , which is measured in pH=7.0 PBS (50 mM) containing 0.1% DMSO. The fluorescence increased dramatically upon the addition of Hg^{2+} and followed a slight blue-shift (11 nm). Simultaneously, the distinct photographs in the absence and presence of Hg^{2+} were taken under a UV lamp (365 nm) (Fig. 6, insert). It is probable that Hg^{2+} -induced desulfurization have taken place. As can be seen in Fig. 7, the fluorescence intensity at 470 nm enhanced upon the stepwise addition of Hg^{2+} and almost reached the plateau when the concentration of Hg^{2+} increased up to 1.0 equivalent. Linear fitting can be achieved according to the relationship of the fluorescence intensity and Hg^{2+} concentration ranging from 0 to 10 μM , which shows a good linear relationship ($R^2=0.9966$) (Fig. 7). The limit of detection (LOD) was estimated to be 45 nM on the basis of EPA ($\text{LOD}=3\delta/\text{slop}$) (Figure S10). As a consequence, Hg^{2+} ions can be detected quantitatively by fluorescence spectrometry method with excellent sensitivity.

(Fig.6 is inset here)

(Fig.7 is inset here)

3.7 The reaction mechanism of the **Cu-CN-S** fluorescence sensor for Hg^{2+} detection.

In light of the fact that a lot of selective sensors for Hg^{2+} have been explored based on irreversible mercury-induced desulfurization that stem from the strong thiophilic affinity of Hg^{2+} ions.⁵² In this work, we suppose thiocarbonyl will be transformed to carbonyl promoted by Hg^{2+} . To verify our assumed principle, the reaction mechanism was studied by ^1H NMR and mass spectra. **CN-O** was isolated from the reacting system and the detailed information was shown in Figure S11. ^1H NMR spectra of **CN-S** (A) and **CN-O** (B) were shown in Fig. 8 and the changes of proton magnetic resonance signal were labeled. As for the mass spectra, the peaks of $[\text{M}+\text{H}]^+$, $[\text{M}+\text{NH}_4]^+$ and $[\text{M}+\text{Na}]^+$ ($\text{M}=\text{CN-O}$) for the reacting system of **Cu-CN-S** with Hg^{2+} were found in Figure S12. The morphology of **CN-O** in aqueous solution (containing 0.1% DMSO) is fiber-like aggregation shown in Figure S13. In addition, as shown in Figure S14 and Figure S15, **CN-O** possesses unusual AIE features and has similar fluorescence emission spectra with the mix of **Cu-CN-S** and Hg^{2+} under the same condition. Thus, a probable mechanism was depicted in scheme 3. Firstly, Hg^{2+} could change the central atom of the complex **Cu-CN-S** by displacing Cu^{2+} promptly, and then desulfurization took place immediately.

(Fig. 8 is inset here)

(Scheme 3 is inset here)

3.8 Time-resolved fluorescence study

To obtain stable fluorescence intensity, the reaction time experiments were

conducted. All measurements were started after 10 s owing to the manipulation time. The response of **CN-S** to Cu^{2+} is rapid. The fluorescence intensity has dropped to minimum value within the manipulation time. A progressive curve was obtained within 20 min and the fluorescence intensity reached to maximum value when 1.0 equivalent of Hg^{2+} was added and the results were shown in Fig. 9. In the absence of Hg^{2+} , free **Cu-CN-S** was intact and no fluorescence increment was noted at all

(Fig. 9 is inset here)

3.9 Interfering fluorescence study

To further testify the interference of **CN-S** for Cu^{2+} and **Cu-CN-S** for Hg^{2+} respectively, various metal ions like Li^+ , Na^+ , K^+ , Mg^{2+} , Ca^{2+} , Al^{3+} , Fe^{2+} , Fe^{3+} , Mn^{2+} , Co^{2+} , Ni^{2+} , Pb^{2+} , Zn^{2+} , Sn^{2+} , Ag^+ , Cd^{2+} , Ba^{2+} and Cr^{3+} were chosen as the interfering ions, some of which have a relatively high concentration in biological tissues or drinking water. In Fig. 10, the experimental results indicated that fluorescence emission of **CN-S** at 492 nm quenched by Cu^{2+} exhibited negligible changes in the existence of the interfering ions. Likewise, there is also no noticeable emission intensity changes in the recognition of Hg^{2+} based on **Cu-CN-S** in the presence of interfering ions and the results were shown in Fig. 11. Thus, it provided a potential application for biological detection and water quality monitoring.

(Fig. 10 is inset here)

(Fig. 11 is inset here)

4. Analysis of Hg^{2+} in real sample

The fluorescent probe **Cu-CN-S** has been validated for practical applications in the determination of Hg^{2+} ions content in three water samples that were collected from Qinghe River in Beijing (sample 1), Weiming Lake in Beijing (sample 2) and tap water (sample 3). Control experiments show that no Hg^{2+} were detected in the three blank samples. When Hg^{2+} was added, fluorescence spectra were recorded and the contents of Hg^{2+} ions were recovered using the linear equation obtained in Fig. 7. Table 1 presents the results and it can be seen that they have good recoveries at the concentrations of 6 μM . In order to further demonstrate the accuracy of this method, the detection in certified reference material of standard solution of Hg^{2+} was carried out according to the analytical procedure. The results were shown in Table 2 and it shows good agreement between the expected and found values. All these data above indicate the proposed method can be used to analyze Hg^{2+} accurately.

(Table 1 is inset here)

(Table 2 is inset here)

5 Conclusion

In summary, we have designed and synthesized **CN-S** which was a single molecular and can be used as a dual analyte fluorescent sensor. The sensor has high selectivity and sensitivity towards Cu^{2+} and Hg^{2+} based on the AIE mechanism. **CN-S** has stronger binding affinity to Cu^{2+} than that of other metal cations, leading to rapid fluorescence turn-off. Most important of all, **Cu-CN-S** can be employed for the

fluorescence turn-on detection of Hg^{2+} , with a low detection limit ($\text{LOD}=45 \text{ nM}$) and good selectivity in aqueous solution based on Hg^{2+} -induced desulfurization mechanism. As a consequence, it was expected that **Cu-CN-S** may provide a potential sample due to its special response for Hg^{2+} .

Acknowledgments

We thank the Science and Technology Innovation Foundation for the College Students of Beijing (No. 13220055), the National Natural Science Foundation of China (No. 20972015), and the Natural Science Foundation of Beijing (No. 2112026) for financial support.

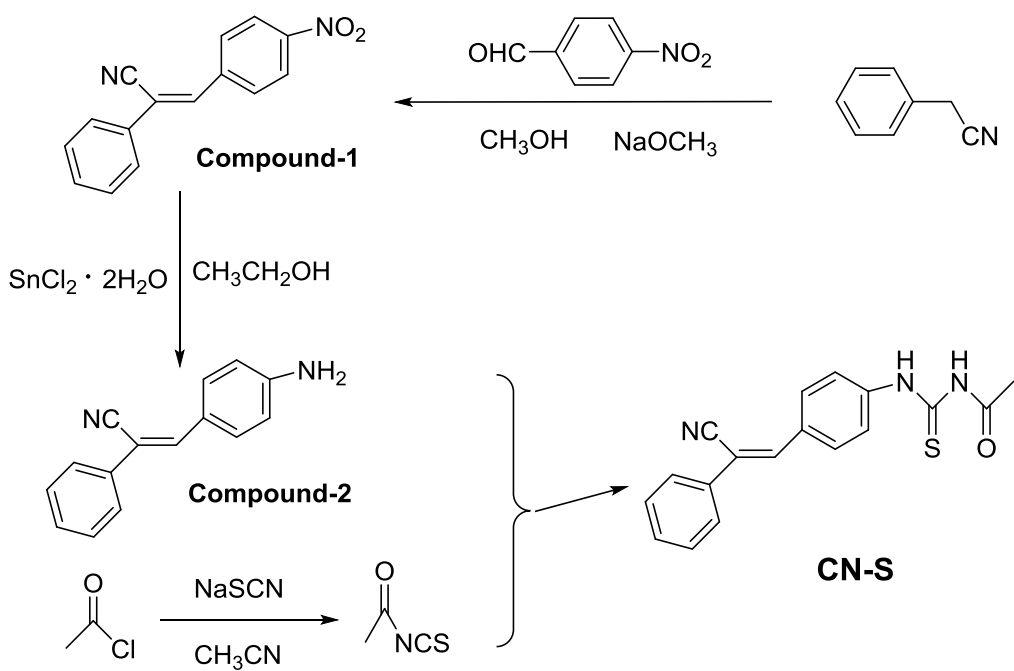
Notes and references

1. A. P. de Silva, H. Q. N. Gunaratne, T. Gunnlaugsson, A. J. M. Huxley, C. P. McCoy, J. T. Rademacher and T. E. Rice, *Chem. Rev.*, 1997, 97, 1515-1566.
2. Q. He, E. W. Miller, A. P. Wong and C. J. Chang, *J. Am. Chem. Soc.*, 2006, 128, 9316-9317.
3. J. H. Kim, J. Y. Noh, I. H. Hwang, J. Kang, J. Kim and C. Kim, *Tetrahedron Lett.*, 2013, 54, 2415-2418.
4. X. Chen, M. J. Jou, H. Lee, S. Kou, J. Lim, S.-W. Nam, S. Park, K.-M. Kim and J. Yoon, *Sens. Actuators, B*, 2009, 137, 597-602.
5. P. Kaur, S. Kaur and K. Singh, *Inorg. Chem. Commun.*, 2009, 12, 978-981.
6. W. Wang, A. Fu, J. You, G. Gao, J. Lan and L. Chen, *Tetrahedron*, 2010, 66, 3695-3701.
7. A. K. Mahapatra, G. Hazra, N. K. Das and S. Goswami, *Sens. Actuators, B*, 2011, 156, 456-462.
8. J. Huang, M. Tang, M. Liu, M. Zhou, Z. Liu, Y. Cao, M. Zhu, S. Liu and W.

- Zeng, *Dyes Pigments*, 2014, 107, 1-8.
9. L. Fu, Y. Xiong, S. Chen and Y. Long, *Anal Methods*, 2015.
 10. S. P. Leach, M. D. Salman and D. Hamar, *Anim. Health. Res. Rev.*, 2006, 7, 97-105.
 11. K. J. Barnham and A. I. Bush, *Curr. Opin. Chem. Biol.*, 2008, 12, 222-228.
 12. R. R. Crichton, D. T. Dexter and R. J. Ward, *Coord. Chem. Rev.*, 2008, 252, 1189-1199.
 13. H. S. Jung, P. S. Kwon, J. W. Lee, J. I. Kim, C. S. Hong, J. W. Kim, S. Yan, J. Y. Lee, J. H. Lee, T. Joo and J. S. Kim, *J. Am. Chem. Soc.*, 2009, 131, 2008-2012.
 14. S. Yin, V. Leen, S. Van Snick, N. Boens and W. Dehaen, *Chem. Commun.*, 2010, 46, 6329-6331.
 15. Y. Ye, Y. Guo, Y. Yue, H. Huang, L. Zhao, Y. Gao and Y. Zhang, *Anal. Methods*, 2015.
 16. P. B. Tchounwou, W. K. Ayensu, N. Ninashvili and D. Sutton, *Environ. Technol.*, 2003, 18, 149-175.
 17. L. Zhang, T. Li, B. Li, J. Li and E. Wang, *Chem. Commun.*, 2010, 46, 1476-1478.
 18. S. Ando and K. Koide, *J. Am. Chem. Soc.*, 2011, 133, 2556-2566.
 19. Z. Gu, M. Zhao, Y. Sheng, L. A. Bentolila and Y. Tang, *Anal. Chem.*, 2011, 83, 2324-2329.
 20. C.-b. Gong, D. Jiang, Q. Tang, L.-h. He, X.-b. Ma and C.-f. Chow, *Anal. Methods*, 2014, 6, 7601-7605.
 21. E. S. Baker, J. W. Hong, B. S. Gaylord, G. C. Bazan and M. T. Bowers, *J. Am. Chem. Soc.*, 2006, 128, 8484-8492.
 22. M. Yu, M. Shi, Z. Chen, F. Li, X. Li, Y. Gao, J. Xu, H. Yang, Z. Zhou, T. Yi and C. Huang, *Chemistry*, 2008, 14, 6892-6900.
 23. Y. Zhao, X.-B. Zhang, Z.-X. Han, L. Qiao, C.-Y. Li, L.-X. Jian, G.-L. Shen and R.-Q. Yu, *Anal. Chem.*, 2009, 81, 7022-7030.
 24. W. Lin, L. Long, B. Chen, W. Tan and W. Gao, *Chem. Commun.*, 2010, 46,

- 1311-1313.
25. S. Hazra, S. Balaji, M. Banerjee, A. Ganguly, N. N. Ghosh and A. Chatterjee, *Anal. Methods*, 2014, 6, 3784.
26. D. E. Kang, C. S. Lim, J. Y. Kim, E. S. Kim, H. J. Chun and B. R. Cho, *Anal. Chem.*, 2014, 86, 5353-5359.
27. C. Zong, K. Ai, G. Zhang, H. Li and L. Lu, *Anal. Chem.*, 2011, 83, 3126-3132.
28. G. Zhang, A. Ding, Y. Zhang, L. Yang, L. Kong, X. Zhang, X. Tao, Y. Tian and J. Yang, *Sens. Actuators, B*, 2014, 202, 209-216.
29. P. Kaur, S. Kaur, K. Singh, P. R. Sharma and T. Kaur, *Dalton Trans.*, 2011, 40, 10818-10821.
30. B. P. Joshi, C. R. Lohani and K. H. Lee, *Org. biomol. chem.*, 2010, 8, 3220-3226.
31. L. N. Neupane, J. M. Kim, C. R. Lohani and K.-H. Lee, *J. Mater. Chem.*, 2012, 22, 4003.
32. M. kumar, N. kumar, V. bhalla, H. singh, P. R. sharma and T. kaur, *org. lett.*, 2011, 13, 1422-1425.
33. X. Li, B. Xu, H. Lu, Z. Wang, J. Zhang, Y. Zhang, Y. Dong, K. Ma, S. Wen and W. Tian, *Anal. Methods*, 2013, 5, 438.
34. Y. Dong, J. W. Y. Lam, A. Qin, Z. Li, J. Liu, J. Sun, Y. Dong and B. Z. Tang, *Chem. Phys. Lett.*, 2007, 446, 124-127.
35. Y. Hong, M. Haussler, J. W. Lam, Z. Li, K. K. Sin, Y. Dong, H. Tong, J. Liu, A. Qin, R. Renneberg and B. Z. Tang, *Chemistry*, 2008, 14, 6428-6437.
36. J. Chen, W. Liu, Y. Wang, H. Zhang, J. Wu, H. Xu, W. Ju and P. Wang, *Tetrahedron Lett.*, 2013, 54, 6447-6449.
37. M. Wang, G. Zhang, D. Zhang, D. Zhu and B. Z. Tang, *J. Mater. Chem.*, 2010, 20, 1858-1867.
38. Z. Liu, W. Xue, Z. Cai, G. Zhang and D. Zhang, *J. Mater. Chem.*, 2011, 21, 14487.
39. H. Bai, J. Qian, H. Tian, W. Pan, L. Zhang and W. Zhang, *Dyes Pigments*, 2014, 103, 1-8.

- 1
2
3
4 40. B.-K. An, S.-K. Kwon, S.-D. Jung and S. Y. Park, *J. Am. Chem. Soc.*, 2002,
5 124, 14410-14415.
6
7
8 41. B.-K. An, D.-S. Lee, J.-S. Lee, Y.-S. Park, H.-S. Song and S. Y. Park, *J. Am.*
9 *Chem. Soc.*, 2004, 126, 10232-10233.
10
11 42. H. Nam, B. Boury and S. Y. Park, *Chem. Mater.*, 2006, 18, 5716-5721.
12
13 43. B. K. An, S. K. Kwon and S. Y. Park, *Angew. Chem. Int. Ed.*, 2007, 46,
14 1978-1982.
15
16
17 44. M. H. Lee, B.-K. Cho, J. Yoon and J. S. Kim, *Org. Lett.*, 2007, 9, 4515-4518.
18
19 45. X. Cheng, Q. Li, J. Qin and Z. Li, *ACS appl. mater. inter.*, 2010, 2, 1066-1072.
20
21 46. Z. Guo, W. Zhu, M. Zhu, X. Wu and H. Tian, *Chemistry*, 2010, 16,
22 14424-14432.
23
24
25 47. K. Tsukamoto, Y. Shinohara, S. Iwasaki and H. Maeda, *Chem Commun.*, 2011,
26 47, 5073-5075.
27
28
29 48. Y. Liu, M. Chen, T. Cao, Y. Sun, C. Li, Q. Liu, T. Yang, L. Yao, W. Feng and F.
30 Li, *J. Am. Chem. Soc.*, 2013, 135, 9869-9876.
31
32
33 49. Y. Xu, Z. Jiang, Y. Xiao, T. T. Zhang, J. Y. Miao and B. X. Zhao, *Anal. Chim.*
34 *Acta*, 2014, 807, 126-134.
35
36
37 50. Y. S. Zheng and Y. J. Hu, *J. org. chem.*, 2009, 74, 5660-5663.
38
39 51. C. Yu, T. Wang, K. Xu, J. Zhao, M. Li, S. Weng and J. Zhang, *Dyes Pigments*,
40 2013, 96, 38-44.
41
42
43 52. Y. Xu, Z. Jiang, Y. Xiao, T.-T. Zhang, J.-Y. Miao and B.-X. Zhao, *Anal. Chim.*
44 *Acta*, 2014, 807, 126-134.
45
46
47
48
49
50
51
52
53
54
55
56
57
58
59
60



Scheme 1. The synthetic pathway of CN-S

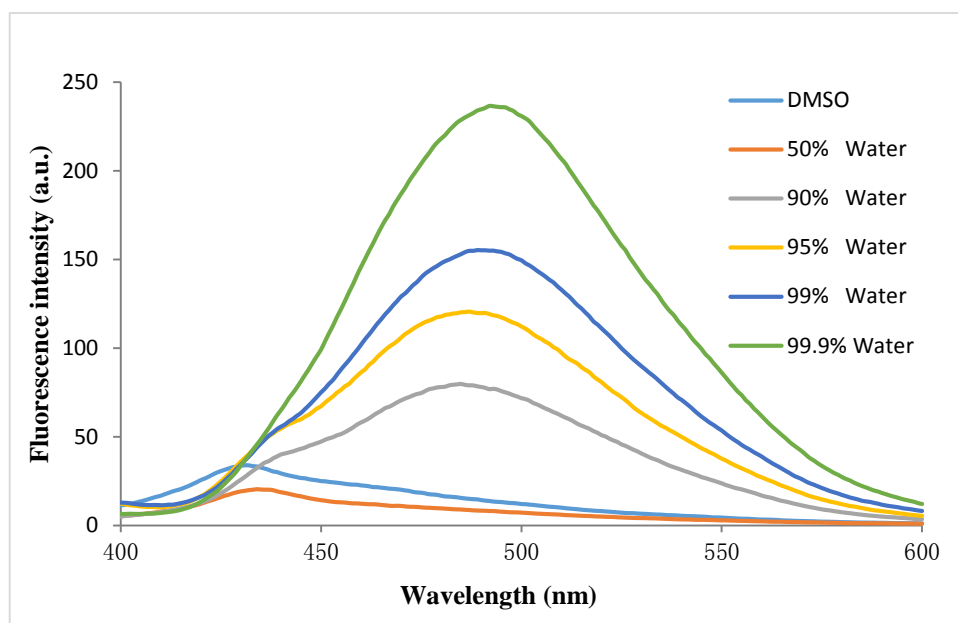


Fig. 1(a) Fluorescent spectra of **CN-S** ($10 \mu\text{M}$) in a DMSO/water mixture (excitation wavelength was 380 nm).

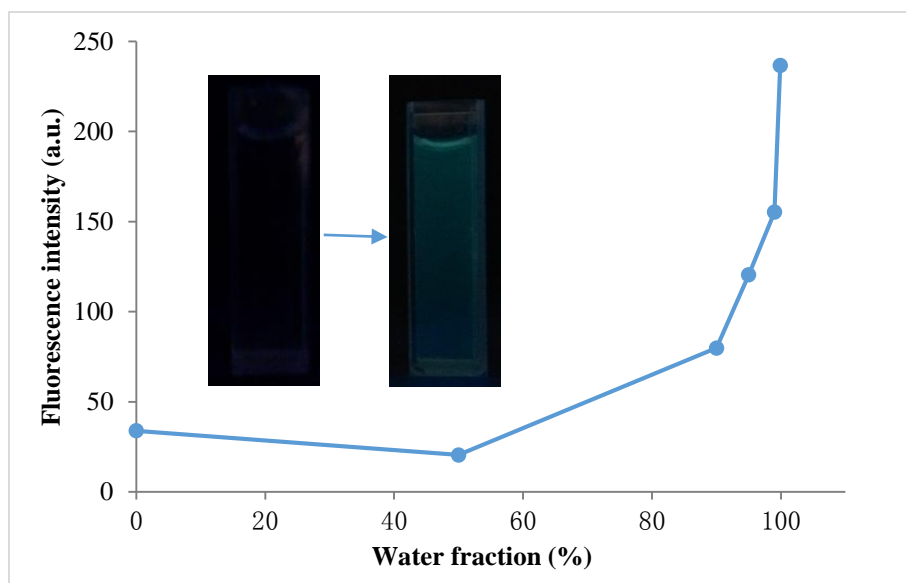


Fig. 1(b) Effect of water volume fraction on the emission intensity of **CN-S** ($10 \mu\text{M}$) in DMSO/water containing 50 mM PBS at pH 7.0. Inset show photographs of **CN-S** ($10 \mu\text{M}$) in dilute DMSO solution and a DMSO/water mixture with a high water fraction under a UV lamp (365 nm). Excitation and emission was at 380nm/492nm respectively.

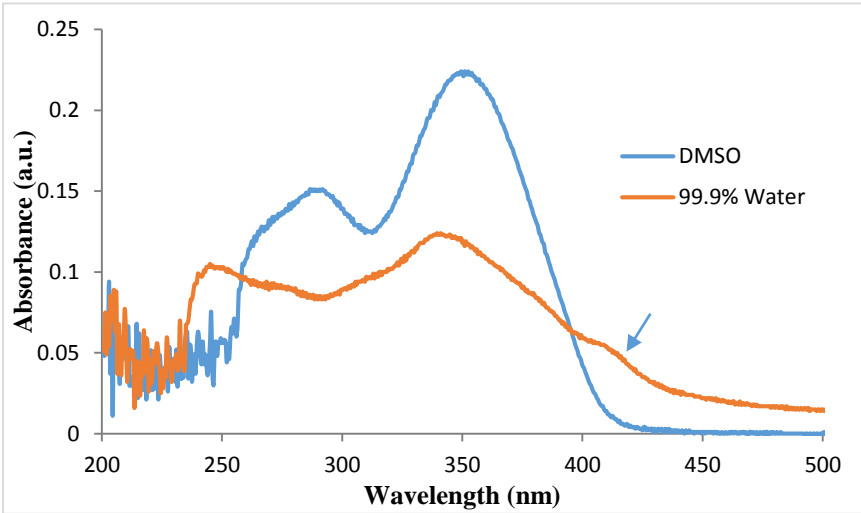


Fig. 2 Absorbance spectra of CN-S (10 μM) in a DMSO–water mixture.

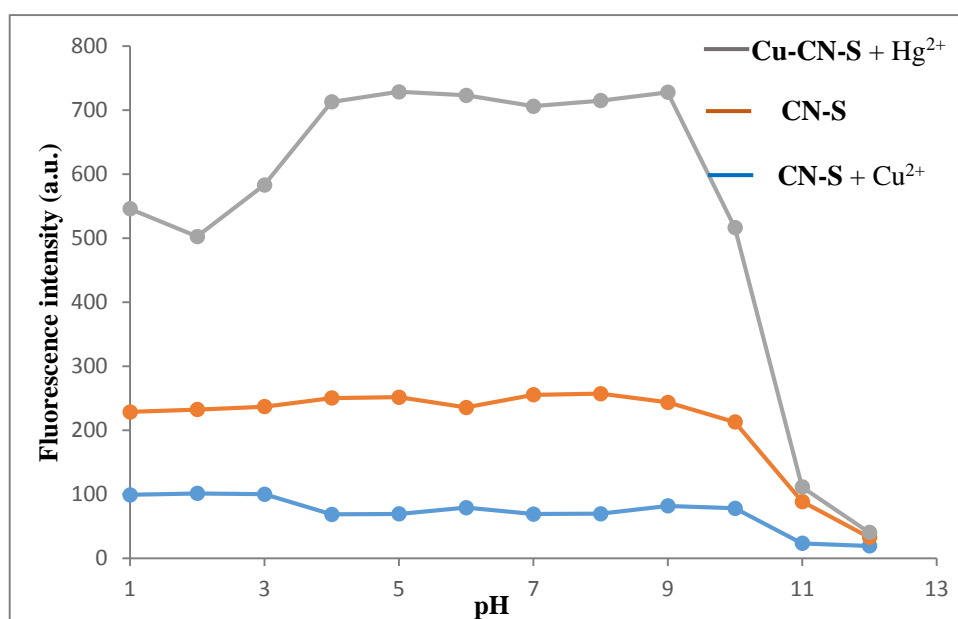


Fig. 3 The effect of pH on fluorescence intensity of **CN-S** (10 μM), **CN-S** (10 μM) and Cu^{2+} (10 μM), **Cu-CN-S** (10 μM) and Hg^{2+} (10 μM). All measurements were taken in 50 mM PBS buffer at pH 7.0 (containing 0.1% DMSO) at 25°C. Excitation and emission were at 380 nm/470 nm.

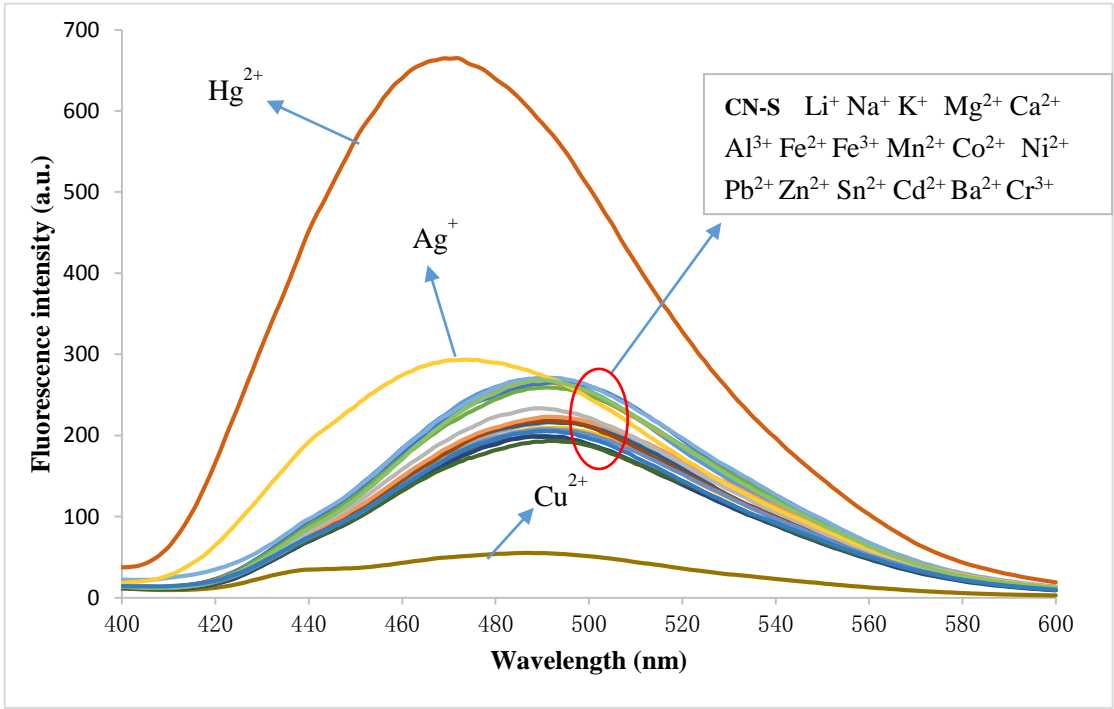


Fig.4 Fluorescence spectra of CN-S (10 μM) in the absence and presence of different common metal ions of Li⁺, Na⁺, K⁺, Mg²⁺, Ca²⁺, Al³⁺, Fe²⁺, Fe³⁺, Mn²⁺, Cu²⁺, Co²⁺, Ni²⁺, Pb²⁺, Zn²⁺, Sn²⁺, Ag⁺, Cd²⁺, Ba²⁺, Cr³⁺, Hg²⁺ separately. All measurements were taken in 50 mM PBS buffer at pH 7.0 (containing 0.1% DMSO) at 25°C. Excitation wavelength was 380 nm.

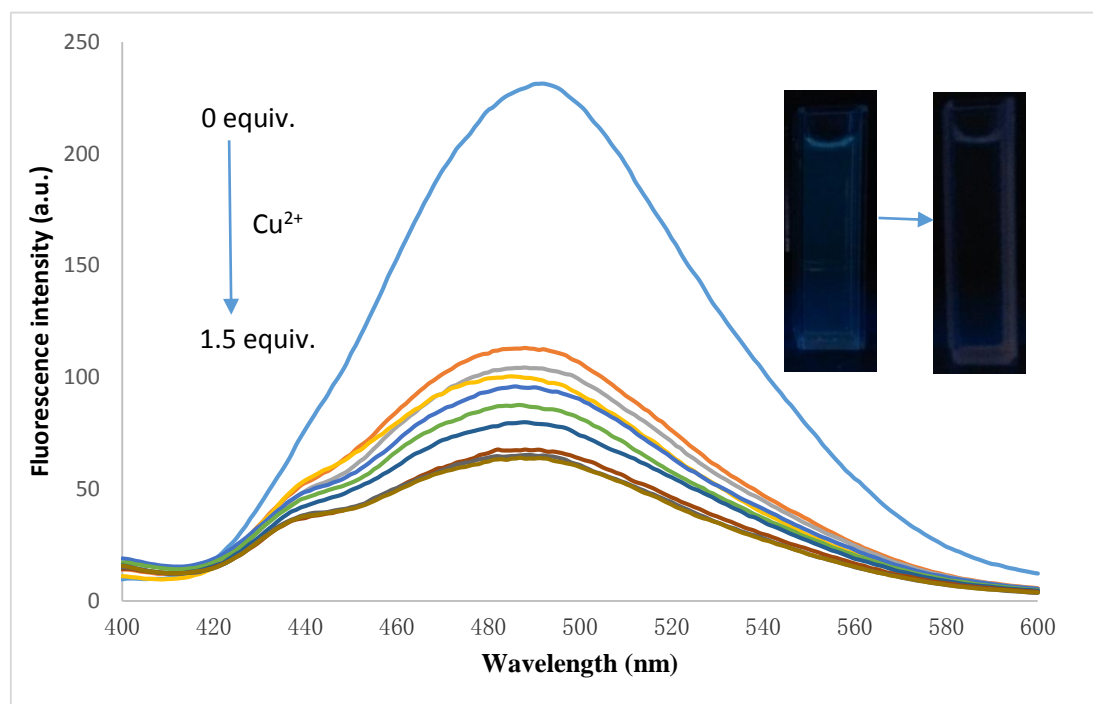
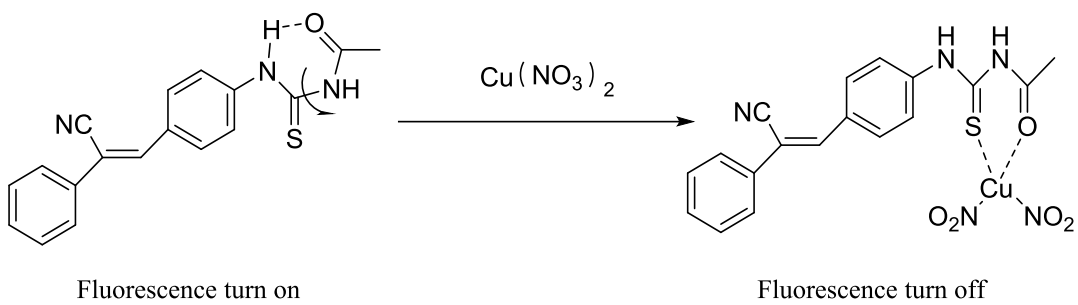


Fig.5 Fluorescence spectra of **CN-S** (10 μM) upon the addition of different concentrations of Cu²⁺ (0, 0.05, 0.1, 0.2, 0.4, 0.6, 0.8, 1.0, 1.2, 1.5 equiv.) in 50 mM PBS buffer at pH 7.0 (containing 0.1% DMSO). All measurements were taken at 25°C. Excitation wavelength was 380 nm. Inset show photographs in the absence and presence of Cu²⁺ (1.5 equiv.) under a UV lamp (365 nm).



Scheme 2. A proposed binding mechanism of **CN-S** with Cu^{2+}

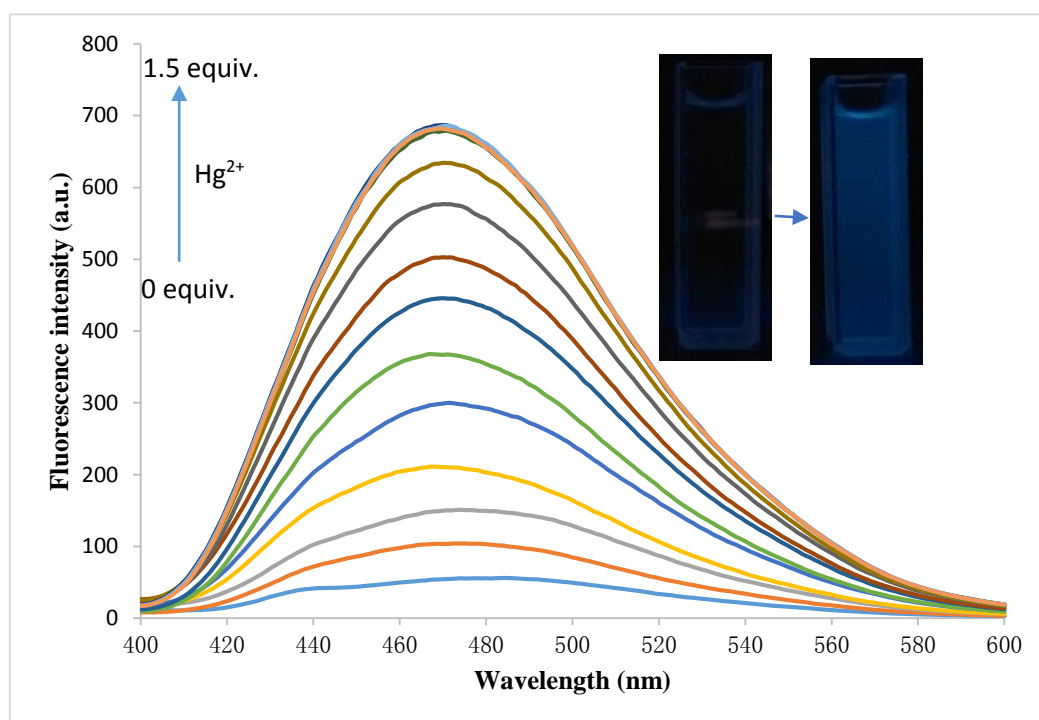


Fig.6 Fluorescence spectra of **Cu-CN-S** ($10\ \mu\text{M}$) upon the addition of different concentrations of Hg^{2+} (0, 0.1, 0.2, 0.3, 0.4, 0.5, 0.6, 0.7, 0.8, 0.9, 1.0, 1.1, 1.2, 1.5 equiv.) in 50 mM PBS buffer at pH 7.0 (containing 0.1% DMSO). All measurements were taken at 25°C . Excitation wavelength was 380 nm. Inset show photographs in the absence and presence of Hg^{2+} (1.5 equiv.) under a UV lamp (365 nm).

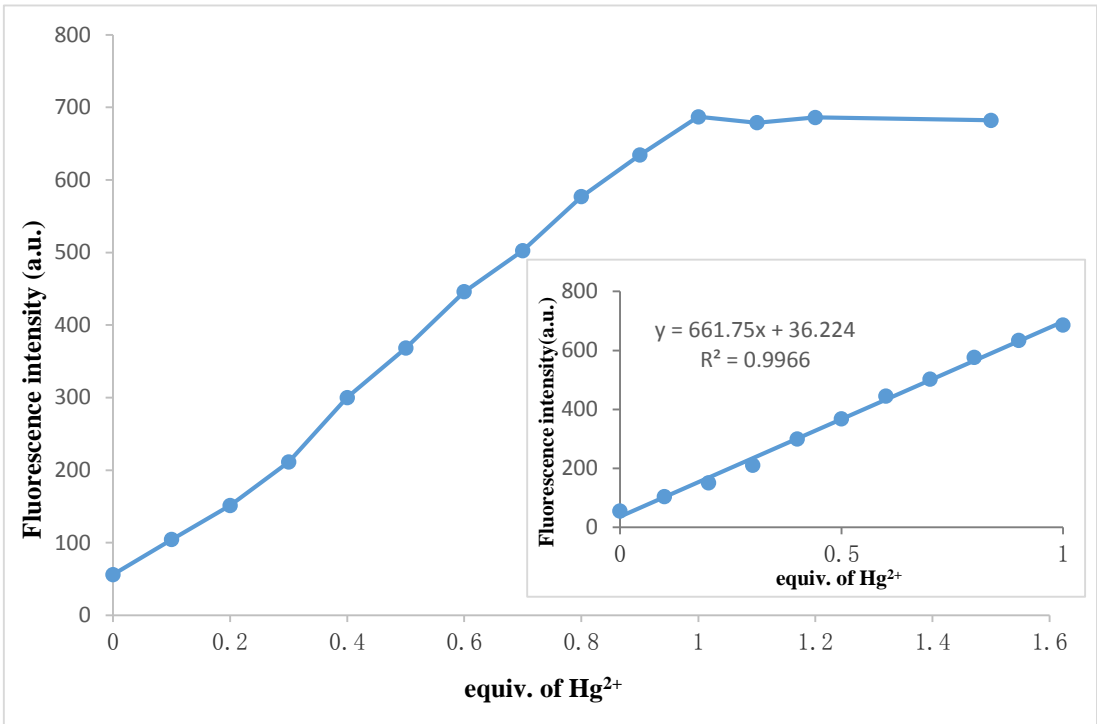


Fig.7 A plot of the fluorescence intensity obtained from the reaction of **Cu-CN-S** (10 μ M) with Hg²⁺ (1.5 equiv.). Inset: the relationship between the fluorescence intensity and Hg²⁺ concentration. All measurements were taken in 50 mM PBS buffer at pH 7.0 (containing 0.1% DMSO) at 25°C. Excitation and emission were at 380 nm/470 nm.

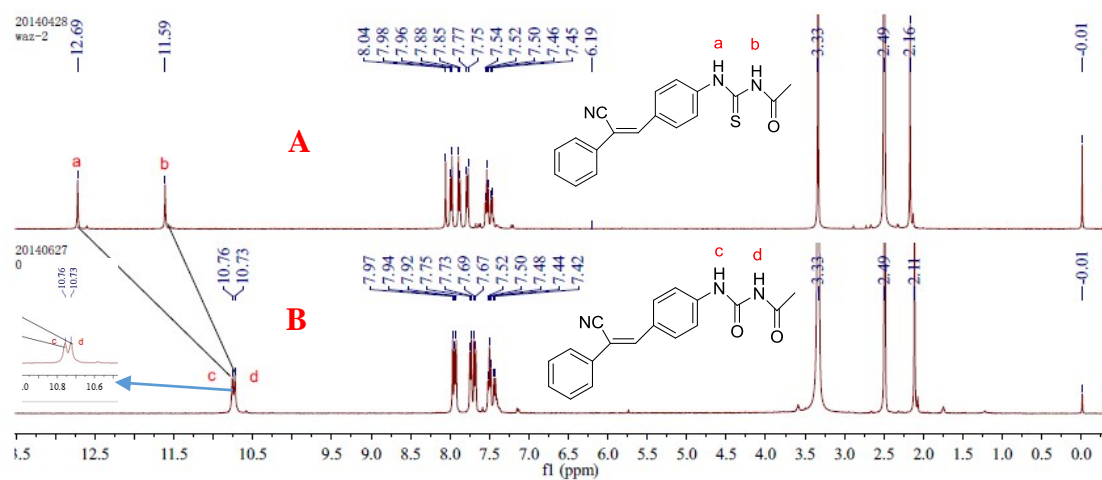
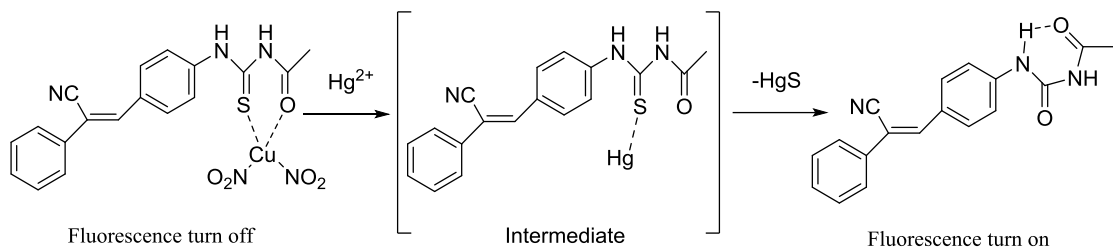


Fig. 8 Partial ^1H NMR spectra of **CN-S**(A) and **Cu-CN-S+Hg $^{2+}$** (B)



Scheme 3. A proposed reaction mechanism of the **Cu-CN-S** with Hg²⁺

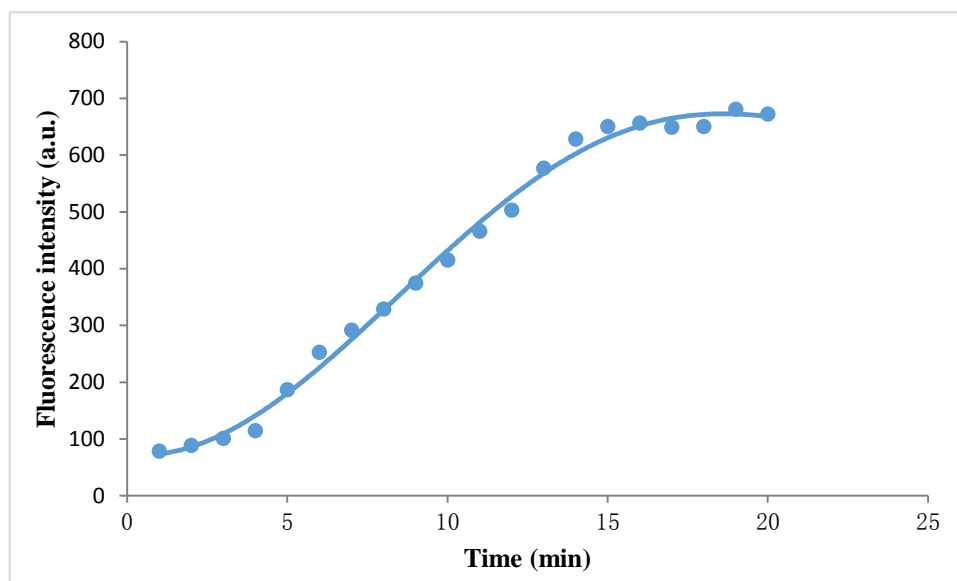


Fig. 9 Time-dependent PL spectra of **Cu-CN-S** treated with Hg^{2+} (1.0 equiv.). All measurements were taken in 50 mM PBS buffer at pH 7.0 (containing 0.1% DMSO) at 25°C. Excitation and emission were at 380 nm/470 nm.

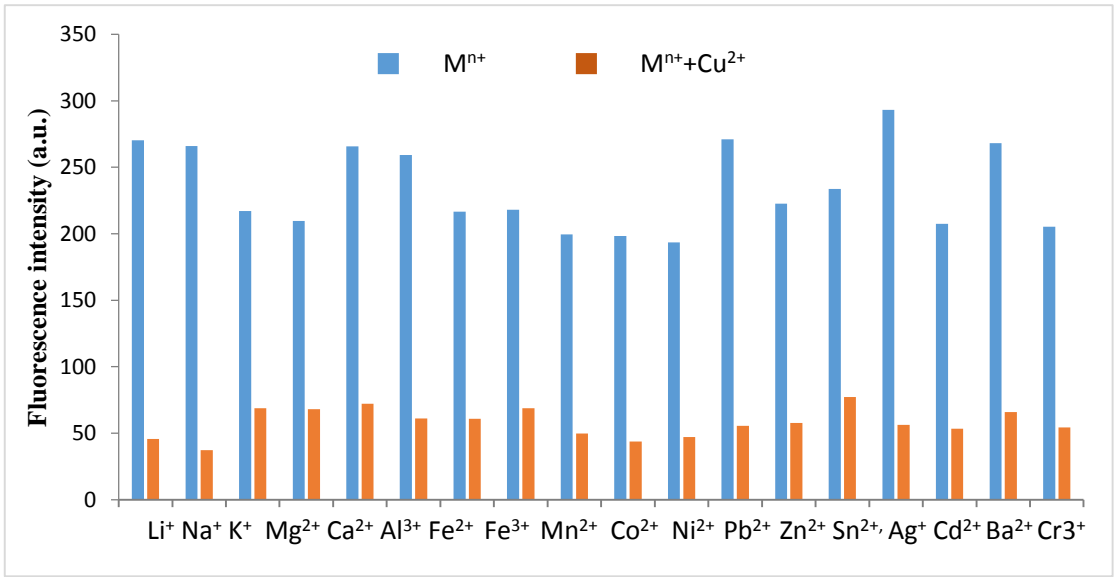


Fig. 10 Fluorescence intensity effects from the reaction of **CN-S** ($10\ \mu M$) with Cu^{2+} in the presence of other metal ions ($20\ \mu M$). All measurements were taken in 50 mM PBS buffer at pH 7.0 (containing 0.1% DMSO) at $25^\circ C$. Excitation and emission were at 380 nm/492 nm.

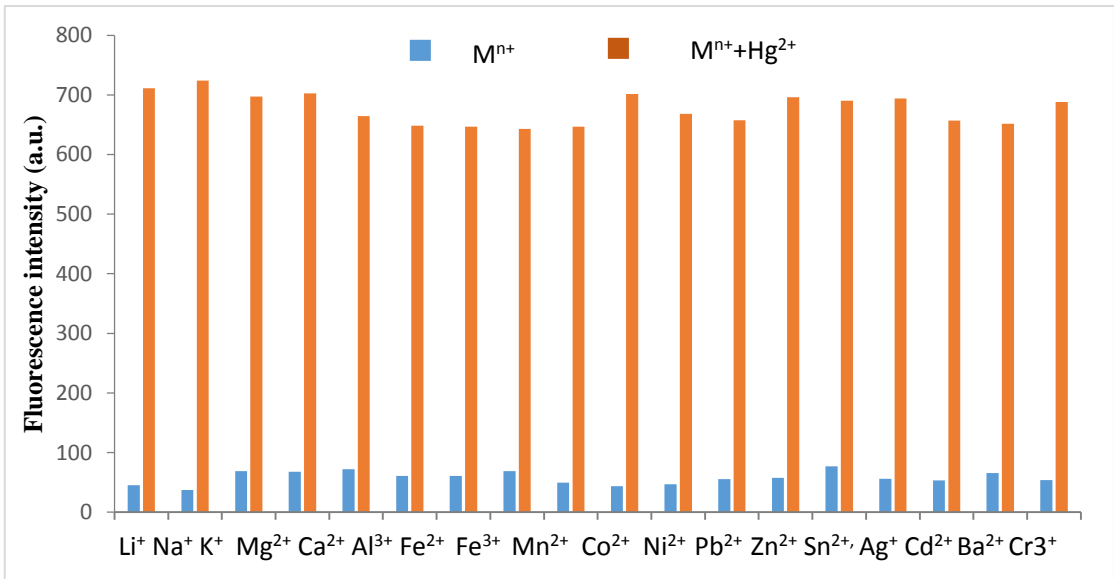


Fig. 11 Fluorescence intensity effects from the reaction of **Cu-CN-S** ($10\ \mu M$) with Hg^{2+} in the presence of other metal ions ($20\ \mu M$). All measurements were taken in 50 mM PBS buffer at pH 7.0 (containing 0.1% DMSO) at $25^\circ C$. Excitation and emission were at 380 nm/470 nm.

Table 1. Detection of Hg^{2+} in real samples.

Sample	Added (μM)	Detected (μM)	Recovery (%)	RSD (%)
Tap water	0	Not detected	-	-
	6	6.27	104.43	5.15
Qinghe River	0	Not detected	-	-
	6	6.12	102.07	4.80
Weiming Lake	0	Not detected	-	-
	6	6.17	102.80	3.04

Table 2. Detection in certified reference material of standard solution of Hg^{2+} .

Sample	Diluted concentration (μM)	Detected (μM)	Recovery (%)	RSD (%)
Standard solution of Hg^{2+}	5	5.09	101.75	2.15